

Model for Electromagnetic and Thermal effect in Mechanical Protection Materials, caused by Electric Currents circulating on non-insulated Buses: Wire Meshes

Daniel Caetano

daniel.caetano@tecnico.ulisboa.pt

Instituto Superior Técnico, Lisboa, Portugal

Abstract—This work intends to study the acceptability of the magnetic induction field originated by the currents flowing in the main busbars of the substation in Electrical Power Plants, studying its influence on the heating of panels or doors made of metallic grids.

In the studied Power Plant, the metallic protection panels and doors are under a variable magnetic induction field (produced by the sinusoidal alternating current circulation in the busbars) where voltage drops occur (electromotive force), causing currents to circulate through the meshes (induced currents), generating undesired heat due to the Joule dissipated power in the conductors that constitute them.

The study will focus mainly on a Power Plant that is in the elaboration and execution phase, to find the best solutions.

Thus, an algorithm was developed to calculate the magnetic induction field, obtained in the regions of the metallic networks, and from this calculation the algorithm determines the distribution of the induced currents in each element of the mesh. Using a thermal study, the developed algorithm allows to obtain the temperature distribution of the net surface.

A simulation program (AQ_Simu) was developed in MATLAB that applies the calculation method capable of solving the magnetic induction field produced by the main busbars, and their distribution and contribution to these unwanted phenomena of temperature, in panels or doors made up of metallic grids (from its location in 3D environment).

Index Terms—Magnetic Induction Field, Induced Currents, Dissipated Power, Heating, AQ_Simu

I. INTRODUCTION

The subject of electromagnetic induction is being studied throughout the years, always with the intention of improving its applications in respect to thermal effects. These reveal clear advantages for this phenomenon in relation to other traditional and widely used methods (losses in electrical resistance, use of gas for heating, etc.).

In this work, it's intended to study the heating effects associated with currents originated by electromagnetic induction. These can be used on practical applications as stated in [1], [2] and [3]: the application in induction coils for hardening of materials, air conditioning of surfaces for the automotive industry, heating off materials in joining processes and even to melt materials producing a state modification (liquid state). In the simplest domestic applications, it has become a method

increasingly used in the so-called thermal induction cooker. In these, an alternating electric current flows through a coil and the resulting alternating magnetic field induces eddy currents in the material. Given the resistance of the material it will turn it into a heater.

However, when these induced currents, which cause the heating of materials, are inconvenient, then it is necessary to study its influence in the temperature raise of the system and try to find ways to minimize it. With this study it is possible to find from geometries to physical conditions adaptable to the different types of electromagnetic and thermal conditions.

A. Problem statement

In certain Power Plants installations due to the presence of magnetic induction fields, created by currents circulating on existing busbars, unnecessary heating has been verified in mechanical protection materials, such as net panels or doors made of metal.

The proximity of main buses to the nets induces, electric currents responsible for the power dissipation by Joule effect, that leads to partial or total heating increase of the constituting materials.

B. Solution

Given the main objective of this study, the way of approach was to treat the Power Plant under study problem as a constitutive interaction in 3D environment.

Knowing the exact location of the main busbars it is possible to obtain the magnetic induction field distribution in any point of the surrounding space. Also, the location and properties of protection materials were important has it clearly influence the undesired heating. Thus, all of the electromagnetic and thermal properties must be granted.

Concerning the metal grids, a model describing how the induced currents were distributed, based on the 3D magnetic field is developed.

Considering the calculus of whole model, a MATLAB software program was develop in order to analyze and produce the desired results in terms of electromagnetic and thermal effects.

C. Document outline

This document starts with a brief description of the main studies and techniques followed in the sequence. This includes also, a description of the problem and the proposed solution.

Then, the second chapter consists in showing the legislation in terms of magnetic field safety and a introduction to the magnetic induction fields.

The third chapter contains the development of the thermal and electromagnetic study for metal grids. This refers to the analysis of a simple grid to generalize the whole content.

Fourth chapter integrates the development of the proposed simulation program AQ_Simu. Here, a presentation is made upon the different features introduced.

In chapter five it is analyzed the Power Plant under study given the metal grids that were installed. Also, sensitivity tests to the Power Plant under study were made with AQ_Simu in order to evaluate the possible heating configurations.

For the last chapter, it summarizes the main achievements, conclusions and analyses at which point this work can be improved in the future.

II. BACKGROUND

In this chapter, a study in the actual state of the concepts and areas related to this work are presented, starting from the electromagnetic approach.

Given the main study, one of the main concerns is the protection of people. This is lead by the undesired heat induction on the metallic protections but also in the intensity of magnetic field itself.

A. Health and Magnetic Induction Fields

The problem of health implications for the exposure to magnetic fields remains a controversial subject. The International Commission on Non-Ionizing Radiation Protection (ICNIRP) has defined a set of reference limits for exposure to electromagnetic fields [4]. The existing legislation in Portugal follows the limits proposed by ICNIRP (although more restricted as shown below). The study of these limitations is important to know in what extent, in the case of Power Plants, the field produced by the main buses is excessive or not and what are the implications for human being.

The patterns of maximum exposure to the magnetic field at low frequencies, following the limits defined by ICNIRP, are those shown in Figure 1 and Figure 2, where f represents the frequency that in this study is 50Hz.

Frequency range	E-field strength E (kV m ⁻¹)	Magnetic field strength H (A m ⁻¹)	Magnetic flux density B (T)
1 Hz–8 Hz	20	$1.63 \times 10^5/f^2$	$0.2/f^2$
8 Hz–25 Hz	20	$2 \times 10^4/f$	$2.5 \times 10^{-2}/f$
25 Hz–300 Hz	$5 \times 10^3/f$	8×10^2	1×10^{-3}
300 Hz–3 kHz	$5 \times 10^3/f$	$2.4 \times 10^5/f$	$0.3/f$
3 kHz–10 MHz	1.7×10^{-1}	80	1×10^{-4}

Fig. 1. Reference values for a temporary exposure to time-varying electric and magnetic fields (taken from [4]).

Frequency range	E-field strength E (kV m ⁻¹)	Magnetic field strength H (A m ⁻¹)	Magnetic flux density B (T)
1 Hz–8 Hz	5	$3.2 \times 10^4/f^2$	$4 \times 10^{-2}/f^2$
8 Hz–25 Hz	5	$4 \times 10^3/f$	$5 \times 10^{-3}/f$
25 Hz–50 Hz	5	1.6×10^2	2×10^{-4}
50 Hz–400 Hz	$2.5 \times 10^2/f$	1.6×10^2	2×10^{-4}
400 Hz–3 kHz	$2.5 \times 10^2/f$	$6.4 \times 10^4/f$	$8 \times 10^{-2}/f$
3 kHz–10 MHz	8.3×10^{-2}	21	2.7×10^{-5}

Fig. 2. Reference values for a permanent exposure to time-varying electric and magnetic fields (taken from [4]).

Given these reference values and considering, as is shown below, the quasi-steady state of the system, ie an operating frequency of 50Hz, the maximum magnetic induction field values for a temporary exposure are 1mT, and for the case of Portugal, this value was increased to 0.1mT, as expressed in Administrative Rule 1421/2004, which adopts Recommendation 519 / EC / 1999 European Council [5]). In the study that follows, these will be taken into account for a correct evaluation of each situation, in terms of the generated magnetic field and for the safety distances that are necessary.

Considering the physical nature of the problem under study, in this case the variation with time of the electromagnetic phenomena, even if this variation is slow, they respect the fundamental equations of Maxwell [6].

$$\text{rot}(\vec{E}) = -\frac{\delta\vec{B}}{\delta t} \quad (1)$$

$$\text{div}(\vec{B}) = 0 \quad (2)$$

$$\text{rot}(\vec{H}) = \vec{J} + \frac{\delta\vec{D}}{\delta t} \quad (3)$$

$$\text{div}(\vec{D}) = \rho \quad (4)$$

In Equations 1 to 4 $E[V/m]$, $B[T]$, $D[C/m^2]$ and $H[A/m]$ respectively represent the vector of electric field, magnetic induction field, electric displacement and magnetic field. $J[A/m^2]$ is the current density vector. Thus, one can assume the quasi-stationary regime since the physical size of the entire structure under study is generally much smaller when compared to the wavelength λ which characterizes the field dynamics. In this case, $\lambda = cT = c/f = 6 * 10^6 m$ given the working frequency of 50Hz. Therefore, for all systems hereafter studied, the steady-state regime presents an approximation that leads to credible study results. By adopting this scheme it is possible to dissociate the capacitive effects associated with electrical induction with inductive effects $\frac{\delta D}{\delta t}$ due to the magnetic induction present in $\frac{\delta B}{\delta t}$. Starting from the phenomena of magnetic induction, characterized by the creation of electric fields E , through the circulation of currents varying in time $J(t)$, the fundamental equations of Maxwell are reduced to:

$$\text{rot}(\vec{E}) = -\frac{\delta\vec{B}}{\delta t} \quad (5)$$

$$\text{div}(\vec{B}) = 0 \quad (6)$$

$$\text{rot}(\vec{H}) \approx \vec{J} \quad (7)$$

Magnetic induction is characterized by the Maxwell-Faraday Induction Law, which allows to translate the appearance of induced electrical voltages, from time-varying magnetic fields. Thus, from equation 5 and using the Stokes Theorem, we obtain equation 8, which will be developed and applied in further chapters of this work.

$$\oint \vec{E} \cdot d\vec{S} = -\frac{d}{dt} \int_{S_s} \vec{B} \cdot \vec{n}_s \, dS \quad (8)$$

III. INDUCED CURRENTS IN METALLIC GRIDS

In this chapter, it is presented the method and approach to solve the problem, concerning metallic grids.

Moreover, describing an example of execution for a simple 3x3 grid, showing the main objective and the necessary components to achieve the goal. This includes the techniques and methodology.

A. Induced currents

For the calculation of currents that are induced in any conductive metal net, a detailed study is necessary from the composition of the material, which constitutes the electric conductors, as well as the insulating material that covers them, to its characteristic geometry. This depends on its length, width and diameter of the conductors, and the length/width of each grid.

Considering any network consisting of n squares arranged along a horizontal line and by m squares arranged along a vertical column, one always have a total number of different currents that makes $2nm + n + m - 4$.

In case of the network of figure 3, we have $n = 3$ and $m = 3$ so that the total number of different currents circulating in the network are $2 \times 3 \times 3 + 3 + 3 - 4 = 20$.

In the characterization of currents, the following conventions are followed:

- 1) The current flow direction is the clockwise direction;
- 2) The first index of each current indicates the number of the horizontal line where the grid is located;
- 3) The second index of each current indicates the number of current in each section of the grid. Note that in each quadrant there are at most four different edges (in the grid squares there are equal edges, for example: $i_{11} = i_{12}$).

The characterization of currents indexes follows the methodology:

- 1) The numbering is always done line by line, and only when one line is fully characterized, the following is done;
- 2) If the current of a section of the next line matches with the current of a section from the previous line, the current in that section retains the designation it had on the previous line.

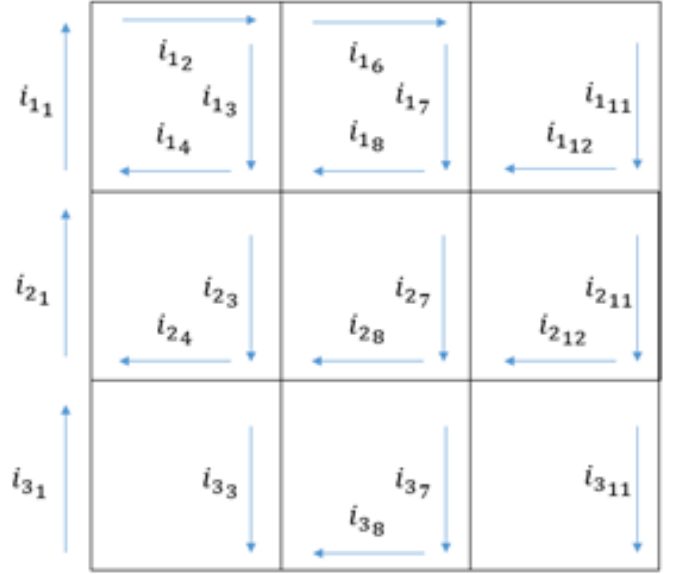


Fig. 3. Example network 3x3 with the different currents and reference to $i_{11} = i_{12}$.

Following these rules it is possible to characterize the set of currents that are necessary to differentiate in the network.

Developing from Maxwell-Faraday's Law of Induction (9), which translates that the electromotive force induced along a closed path is equal to the symmetric one of the derivative of linked magnetic flux with that path.

$$\oint \vec{\beta} \cdot d\vec{l} = \frac{-d\psi(t)}{dt} \quad (9)$$

Therefore:

$$\Delta U(t) = \frac{-d}{dt} \int_S \vec{B} \cdot \vec{n}_s \, dS \quad (10)$$

Thus, taking into account the problem under study and considering as an example the grid of Figure 3, where currents $i_{11}, i_{12}, i_{13}, i_{14}$ circulate, one can obtain in complex notation:

$$R_{troco}(\overline{I_{11}} + \overline{I_{12}} + \overline{I_{13}} + \overline{I_{14}}) = -j\omega \overline{B_{med}} S \quad (11)$$

Where $N = 1$ and S represents the section according to which the magnetic field crosses the concerned grid. $\overline{B_{med}}$ is the sum of the transversal component of each magnetic induction field value from the three busbars in the middle point of the grid square. Each section of the grid is characterized by a resistance, R_{troco} , which depends on the size and material of the mesh.

In this case, we have the vector of currents in complex amplitude given by $\vec{I} = [\overline{I_{11}}, \overline{I_{13}}, \overline{I_{14}}, \overline{I_{16}}, \overline{I_{17}}, \overline{I_{18}}, \overline{I_{111}}, \overline{I_{112}}, \overline{I_{21}}, \overline{I_{23}}, \overline{I_{24}}, \overline{I_{27}}, \overline{I_{28}}, \overline{I_{211}}, \overline{I_{212}}, \overline{I_{31}}, \overline{I_{33}}, \overline{I_{37}}, \overline{I_{38}}, \overline{I_{311}}]$.

For the calculation of these currents the superposition method is used, that is, nine operating modes are considered, each of which is characterized by a magnetic induction field $\overline{B_{med}} \neq 0$ in a grid square and $\overline{B_{med}} = 0$ in all others.

The current in each section is obtained by adding the results corresponding to the nine operating modes: continuing

with the network example 3x3, one calculates the complex amplitude of the current i_{11} , corresponding to the mode of operation in which only the value of $\overline{B}_{med} \neq 0$ is considered in the center square of row one and column one. The equation 12 results from the equation 9 with the result in form of complex amplitude, that can be also seen in figure 4.

$$\overline{I}_{11} = -\frac{j\omega\overline{B}_{med}S}{R_{i_{11}} + Req_{i_{11}}} \quad (12)$$

$R_{i_{11}}$ is the resistance of path current and $Req_{i_{11}}$ is the equivalent resistance of the metallic grid seen from the nodes where the current flows.

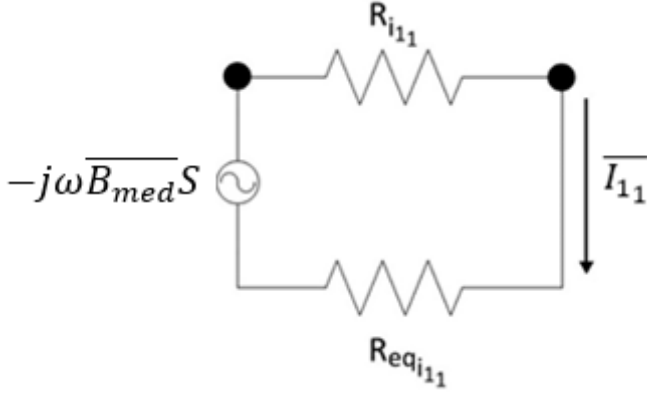


Fig. 4. Resistance seen from the terminals of the current to be calculated

After, the method proceeds calculating the remaining currents due to the same $\overline{B}_{med} \neq 0$. When it concludes, it is necessary to use the knowledge of the grid and for each of the 9 modes, calculate the contributions that the $\overline{B}_{med} \neq 0$ have in the rest of the network.

B. Magnetic Induction Field

For calculating the magnetic induction field in any point (in particular for the middle point of each grid square) it was followed the procedure in [7] which is based on the Biot-Savart law. With this approach it's possible to calculate, in any point, the magnetic induction field value from the three busbars conductors (adding in each point the individual contribution).

C. Equivalent resistances

As a result of equation it is necessary to know the equivalent resistances seen from all 2 nodes of the grid. As so, given the fact that the induced currents are a consequence, the following characterization differs.

To characterize the same network, one use the following nomenclature [8]:

- 1) The potential at point ij is V_{ij} ;
- 2) If ij and kl are neighbors, the equation $|i-k|+|j-l| = 1$ is true (ie, they are adjacent). The conductance between two connected nodes ij and kl is G_{ijkl} ;
- 3) The current injected into the node ij is called I_{ij} .

Assuming that the total sum of the currents for all nodes equals zero, following again the Kirchoff law for the currents,

it follows that to know the resistance between two chosen points in the network it is necessary to respect the equation 13.

$$G_{ij+i_{1j}}(V_{ij} - V_{i+i_{1j}}) + G_{ijj-1j}(V_{ij} - V_{i-1j}) + G_{ijj+1}(V_{ij} - V_{ij+1}) + G_{ijj-1}(V_{ij} - V_{ij-1}) = I_{ij} \quad (13)$$

That is, by using the conductance in each branch and the tension applied, one have by the Kirchoff law of nodes, the current I_{ij} injected in each node.

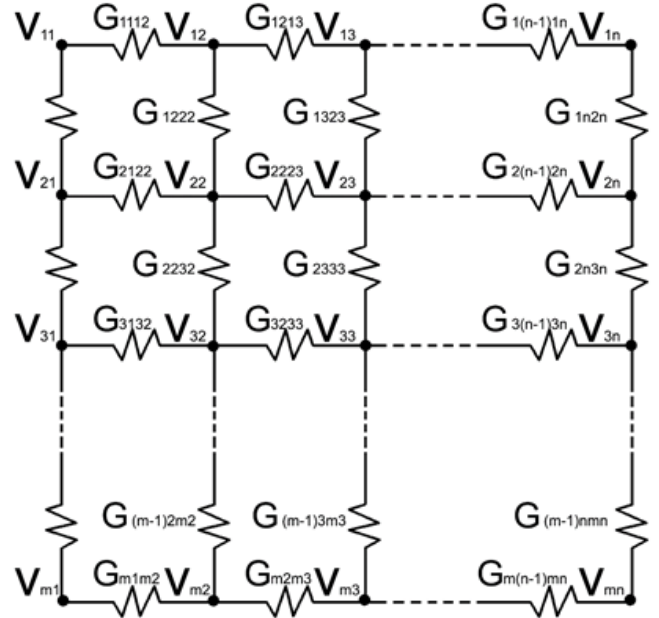


Fig. 5. Network of $n \times m$ grid boxes with resistances in each section (adapted from [8])

D. Heating Transfer

Consider the diagram of figure 6 where the constituent layers are represented. First one is the thermal resistance R_{cond} representing the resistance of the conductor (that is neglected considering no change in temperature inside), R_{isol} represents the insulation material varnish/plastic paint from the network and R_{conv} represents the surrounding air.

Thus, from a permanent analysis (without the influence of the thermal capacitances) the heat transfer takes place from the conductive material, is transmitted by conduction to the insulation one and subsequently by convection into the air. These heating transmissions originate different temperatures, which will be evaluated in terms of heating the network, which are T_1 for the temperature at the conductor, T_2 at the insulation material and $T_{\infty,1}$ representing the ambient temperature in steady state. The final thermal resistance resulting from the system will be the sum since these are in series, obtaining:

$$R_{Termica\ Total} = R_1 + R_2 = R_{isol} + R_{conv} \quad (14)$$

As shown in figure 7 there are different layers that should be considered when dealing with conductors plastic/varnish cover. With this it's possible to obtain the following equations

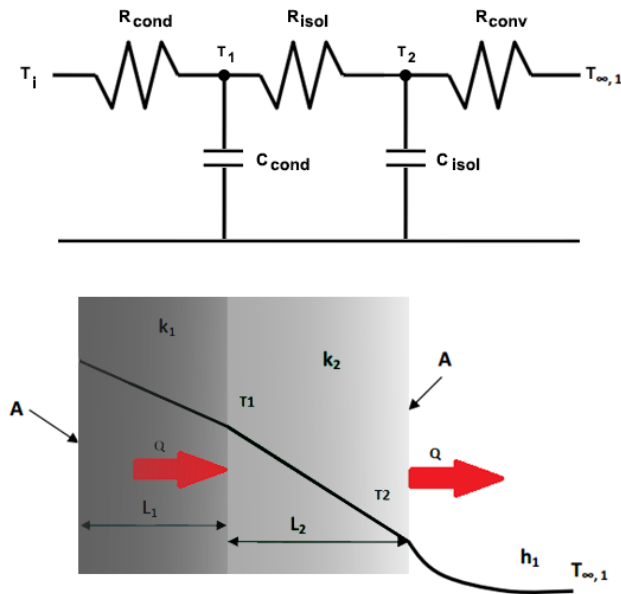


Fig. 6. Diagram of heat transfer with different thermal resistances (adapted from [9])

15 and 16 referring the thermal process [9]. After considering a dynamic regime [10] it is possible to also include the thermal capacitances influence and obtain the total generated heat for temperatures the T_1 and T_2 .

$$R_{\text{Isol}} = \frac{\ln\left(\frac{r_2}{r_1}\right)}{k_2 2\pi L} \quad (15)$$

$$R_{\text{Conv}} = \frac{1}{h_1 A} \quad (16)$$

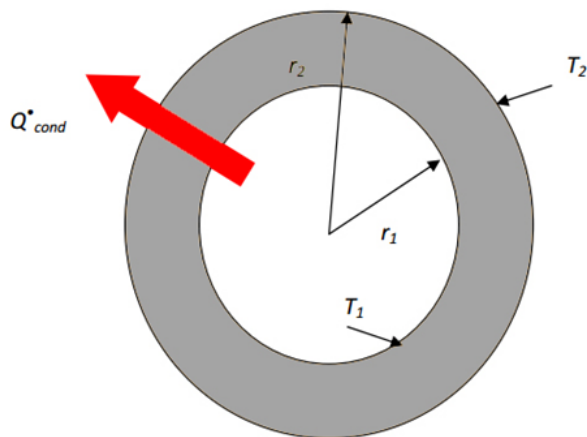


Fig. 7. Representation of the conductor with an insulation layer (adapted from [9])

IV. AQ_SIMU

In this chapter, it is presented the developed MATLAB [11] program AQ_Simu.

Figure 8 depicts the user interface window, where it is possible to enter the necessary data for the calculations, choose the desired results and where some results are presented after the calculations.

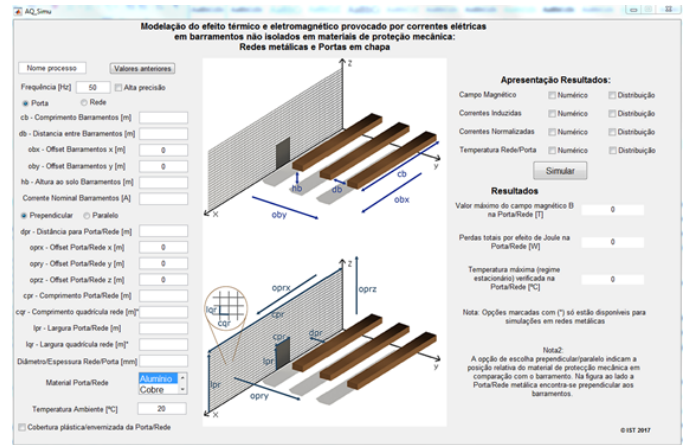


Fig. 8. AQ_Simu GUI

For the program to be able to do the calculations it is necessary to enter the position of the metallic networks, as well as the location of the busbars (in 3D environment). Also, the user has to indicate the working frequency, the length of the buses, the distance between them, the distance to the protective material and the nominal current.

Concerning the thermal effects, one should select the protective material composition, the diameter, the existence of a varnish protection and the ambient temperature.

For results (the ones used later in this study), they are separated into "numeric" and "distribution". With the first one, the user has access to a representation in terms of numeric values for the network, with either the RMS values of transversal magnetic induction field at each calculated point, or the RMS value of currents induced in each branch, or the resulting values of temperature. With the second option the user has a graphical representation of the grid in terms of the distribution RMS values for the magnetic induction field at each calculated point, the distribution for the RMS induced currents in each branch or also a thermographic recording.

V. RESULTS

In this chapter, it is presented the results for simulation with AQ_Simu. This study was made for the requirements data and then for sensitive parameters, testing the program boundaries and Power Plant project execution.

A. Power Plant under study

Tests were carried out for the network panels (PAR) of the installation. In the first case, it is considered a network grid with the dimensions of 1 meter per 1 meter. This is assumed to be centered with the height of the busbars (2 meters high) and also centered in length, meaning that for the 13 meters long busbars, the grid is at 6.5 meters. With this approach, it is possible to test the possibility of safety and heating issues. The distance between the busbars is 0.75m and for the grid is

0.9m. The grid is also considered to be in the xz plane made of iron as one can see in the figure 9.

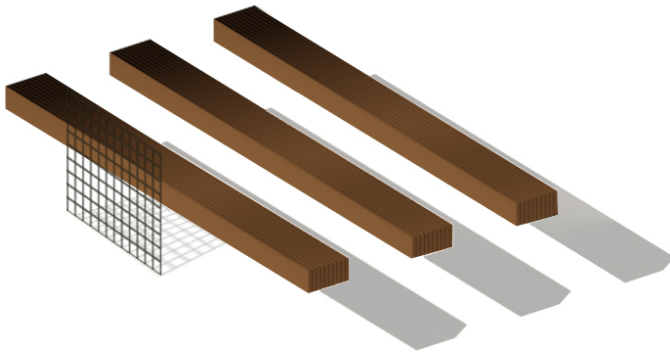


Fig. 9. Relative position PAR for first study in xz plane

PARs have the following characteristics:

- 1) Electrowelded net without plastic cover;
- 2) Diameter of the conductors 2.1mm;
- 3) Width of each grid 25mm;
- 4) Height of each grid 25mm.

Given this dimensions and using the installation parameters for the remaining fields, its obtained the results in figure 10. In this sense, given the relative position of the network grid along with respect to the buses (as so, in the xz plane), the maximum RMS value of the total magnetic induction field close to $1mT$, which represents, according to the ICNIRP recommendations, a value close to the maximum for a temporary exposure. This means that the access and maintenance of these buses should be made by specialized personnel, with adequate protective equipment to minimize potential risks. It may also be noted that this type of configuration (PAR) will not suffer from prolonged heating over time, as the Joule losses are low and the maximum steady state temperature, is practically the ambient temperature considered ($20^{\circ}C$).

Resultados	
Valor eficaz máximo do campo de indução magnética transversal B na superfície da Rede [T]	0.000557089
Perdas totais por efeito de Joule na Rede [W]	0.252659
Temperatura máxima (regime estacionário) verificada na Rede [°C]	20.1697

Fig. 10. Results for PAR of Power Plant under study

In a more detailed evaluation, it is verified that the RMS values of the magnetic induction field, given in figure 11, has a higher intensity in the upper and lower periphery of the grid. As so, at the center of the grid, the transversal component of magnetic induction field is zero. The maximum intensity

RMS value registered in the grid is close to $0.56mT$ (this value represents the transversal component to the grid only).

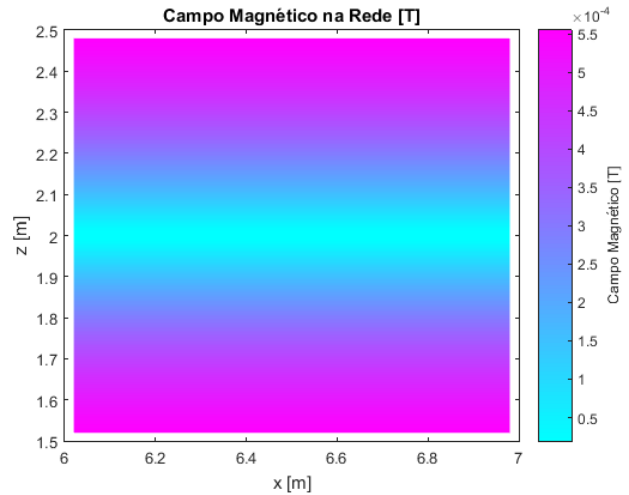


Fig. 11. Magnetic Induction Field distribution in PAR

As for the induced currents in this network topology (figure 12), its distribution is made symmetrically throughout the PAR (contributing to this fact its perfectly centered spatial position with the busbars). However, it shows a higher intensity in the upper and lower part of the network, reaching a maximum of about 1.1A RMS. In this regions is where the magnetic induction field also, has its highest values. The Joule losses are still quite low (about $250mW$) and therefore, as far as the temperatures are concerned, this is close to the ambient temperature. The highest values being recorded are in the upper and lower boundaries of the grid as depicted in figure 13.

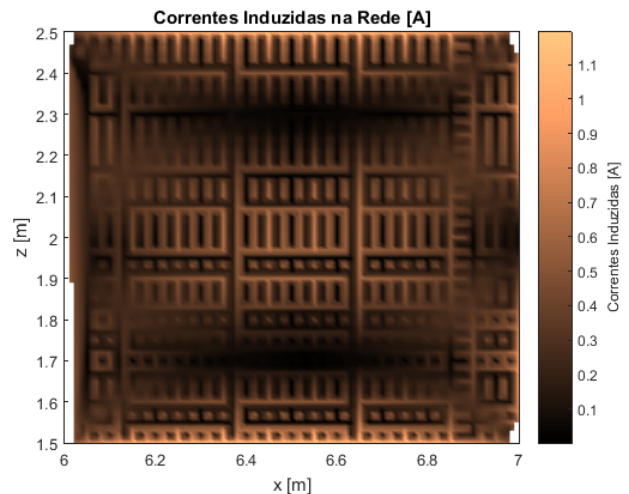


Fig. 12. Currents RMS values distribution in PAR

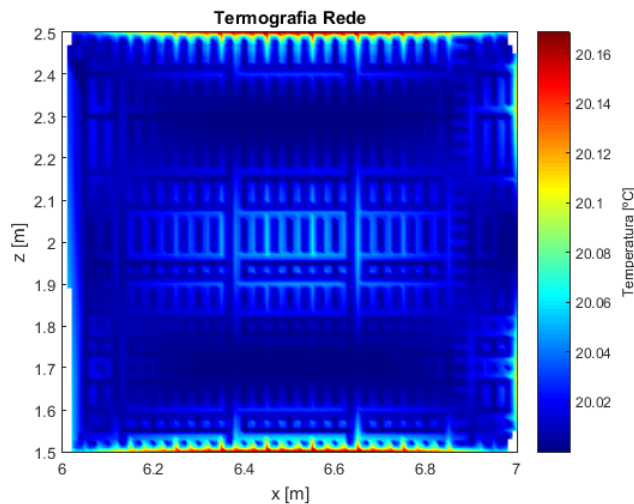


Fig. 13. PAR temperature distribution

In a new configuration for the PAR, it is now considered the same circumstances as the previous test but now the grid is over the busbars (at the same distance of 0.9m and centered at 6.5 meters) as one can see in the figure 14. In this situation it is expected that the values of the induced magnetic field are now superior.

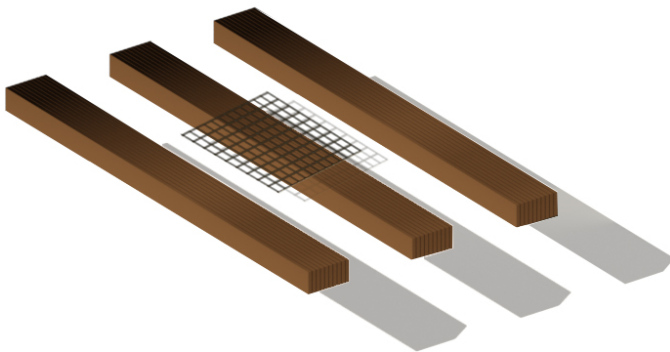


Fig. 14. Relative position PAR for first study in xy plane

Given the same dimensions and installation parameters, its obtained the results in figure 15. Now, even the maximum RMS value of the transversal magnetic induction field is over $1.4mT$, which represents, a value higher than the permitted one for a temporary exposure. With this type of configuration for PAR, the higher exposure to magnetic induction field results in a greater power losses by Joule effect, reaching almost $5W$. The maximum steady state temperature, is more pronounced and has an increase of more than $2^{\circ}C$.

For more detailed evaluation, it is verified that the RMS values of the magnetic induction field are much higher than the previous situation and that the distribution is much more homogeneous, given in figure 16. Now, with the grid position in the xy plane, there are no zero RMS values for the transversal magnetic induction field in the PAR.

The induced currents in this new PAR simulation (figure 17), reveals a more homogeneous too distribution throughout

the PAR (contributing to this fact its perfectly centered spatial position over the busbars). In this case the RMS values for the currents reach more than $4A$.

The Joule losses are about $5W$ and therefore, the temperatures increases around the periphery of the grid as depicted in figure 18.

Based on the results obtained, it can be concluded that there is no heating in the the metallic networks of this installation under study.

Resultados	
Valor eficaz máximo do campo de indução magnética transversal B na superfície da Rede [T]	0.00149022
Perdas totais por efeito de Joule na Rede [W]	4.97019
Temperatura máxima (regime estacionário) verificada na Rede [°C]	22.3886

Fig. 15. Results for PAR of Power Plant under study (2)

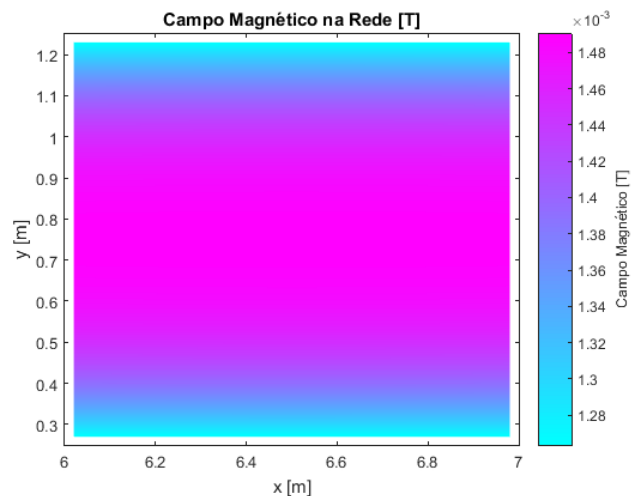


Fig. 16. Magnetic Induction Field distribution in PAR (2)

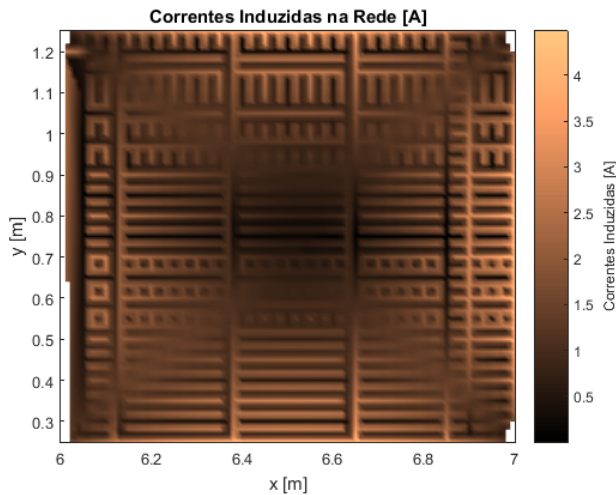


Fig. 17. Currents RMS values distribution in PAR (2)

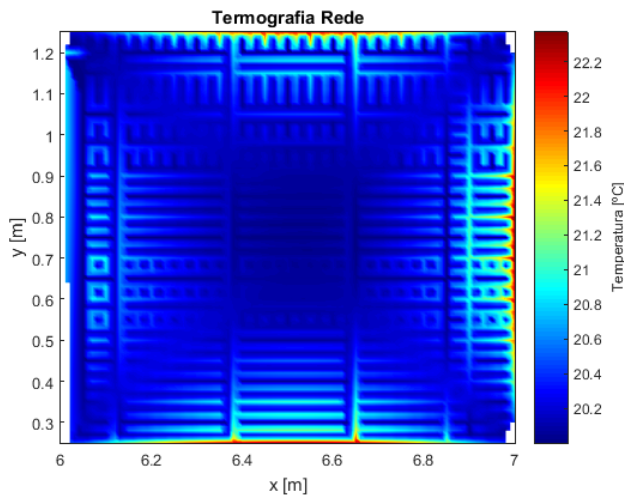


Fig. 18. PAR temperature distribution (2)

B. Sensitivity studies

Taking into account the results obtained for the plant under study, it is important to study the limits for which the safety for people, or even for the purpose of undesired heating, is exceeded.

Therefore, it is necessary to test the variables that are directly or indirectly related to these factors. In this case, the influence of several parameters such as the distance between the busbars of the plant, the distance of the busbars to the metallic protection net, the size of each grid square, the diameter of the conductors of the networks, the effect of existence plastic/varnished cover in the conductors of the metallic protection network and different materials in the constitution of the metallic networks.

1) *Distance between busbars*: When increasing the distance between busbars, the influences to each others disappear and it is considered only one busbar. As so, the RMS values of the magnetic induction field increase. On the other hand it has to be made a study for the minimum distance between them, taking into account the possibility of electrical failures and the

electromagnetic forces that could be generated. In figure 19 is depicted the RMS value of the total magnetic induction field in the grid at 0.9 meters from the busbars (xz plane) considering the distance between busbars.

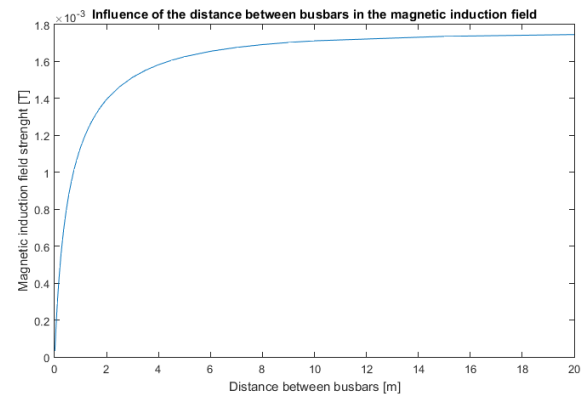


Fig. 19. Distance between busbars results

2) *Distance to the grid*: Considering the distance between the busbars and the grid, it is expected that when reaching the zero distance (excluding electrical failures), the temperature rises to the maximum possible values. This occurs due to the increase in magnetic induction field exposure. As an results example, consider in figure 20 a metallic door (2.4 meters height and 0.6 meters width) that is at the 0.1 meters from the busbars. This door is considered also to have not squares, but rectangular shape grid (80mm height and 40mm width) 4mm diameter thick. This results shows an immense increase in temperature giving it a maximum value close to $860^{\circ}C$.

Resultados	
Valor eficaz máximo do campo de indução magnética transversal B na superfície da Rede [T]	0.00770291
Perdas totais por efeito de Joule na Rede [W]	472.535
Temperatura máxima (regime estacionário) verificada na Rede [°C]	859.662

Fig. 20. Results for 0.1 meters distance to the grid

3) *Dimension of square grids*: For the same grid dimensions, when reducing the number of square grids it is increased the area in which the transversal magnetic induction field, crosses each square grid. When this occurs, the electromotive force will be much higher resulting in induced currents that have bigger value. Given this fact, the total power dissipation increases as so the temperature.

The study was made considering the same PAR from the Power Plant under study (one meter width and one meter height) and reduce the number of square grids to a minimum of 3x3 (a total of 14 combinations). In this last case the grid is similar to the one from figure 3.

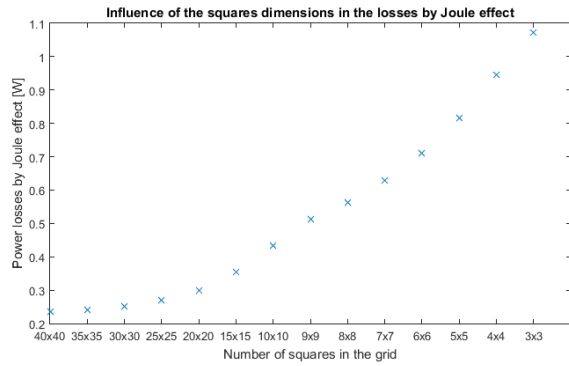


Fig. 21. Results for number of squares influence in power dissipation

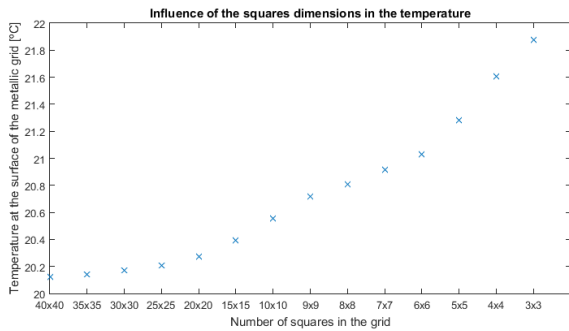


Fig. 22. Results for number of squares influence in maximum temperature

The results are depicted in figure 21 and 22. This results shows a clear increase in both power dissipation by Joule effect and temperature (around 10%).

4) *Conductors diameter*: Considering an improvement in conductors diameter is the same as considering an increase in cross section. Higher the cross section means that there is a decrease in the total conductor resistance and that the current that flows in each segment of the grid will increase. This will lead into higher dissipation power and as an effect to a greater increase in temperature as shown in figures 23 and 24.

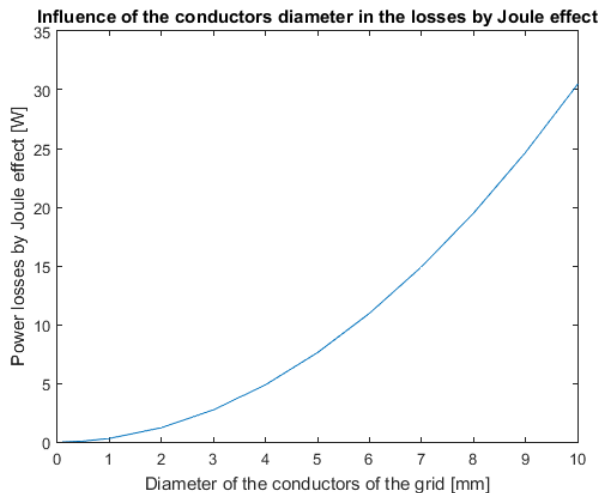


Fig. 23. Results for conductor diameter influence in power dissipation

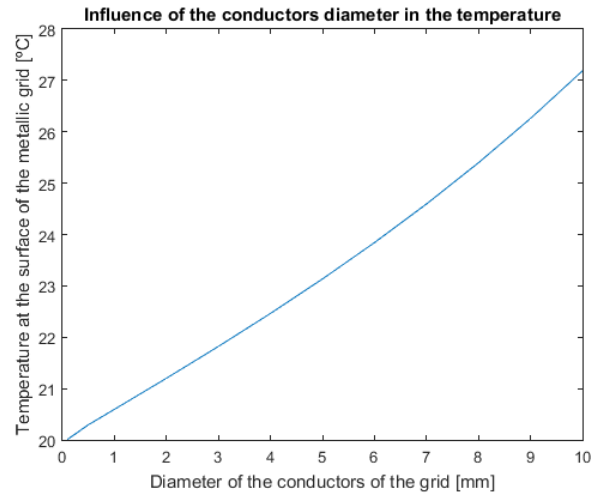


Fig. 24. Results for conductor diameter influence in maximum temperature

5) *Plastic/Varnish cover*: For the plastic cover of a conductor, as it is considered an insulator from an electric point of view, it is a clear advantage in terms of people safety. Also, it can prevent oxidation processes (like the case of Iron). However in particular installations where conductors would increase more their temperature this layer of protection can result in negative effects, rising even more the conductor temperature, when comparing to the ones without it. In figure 25 there is the results of a simulation with (left) and without (right) plastic/varnish cover on the surface of the grid.

Resultados		
Valor eficaz máximo do campo de indução magnética transversal B na superfície da Rede [T]	0.000614581	0.000614581
Perdas totais por efeito de Joule na Rede [W]	3.25259	3.25259
Temperatura máxima (regime estacionário) verificada na Rede [°C]	22.3871	22.3846

Fig. 25. Results comparison for plastic/varnish cover

6) *Constitutive material*: Every material has his own thermal, magnetic and electric properties. This can influence all the desired study because it's directly related to the induced currents and dissipated power capabilities. As seen in table I, for the same inputs the difference in temperature can rise more than 60%.

TABLE I
COMPARISON BETWEEN DIFFERENT MATERIALS

Material	Total losses by Joule effect [W]	Maximum Temperature [°C]
Aluminum	17.8611	29.4816
Cooper	28.1737	36.0630
Iron	4.8745	22.4655
Zinc	8.0223	24.1156

VI. CONCLUSION

The objective of this work was the development of a thermal-magnetic model that allows to determine the intensity and distribution of induced currents in network grids and doors and the losses by Joule effect. Based on the losses, the thermal model allows to obtain the temperature distribution in these elements. In this study, the maximum values reached by the field were also analyzed and are compared with the exposure limits to the magnetic induction fields given by ICNIRP.

For the safety of people and the installation, a very high level of requirements are needed. Therefore an effective and concrete study should be implemented to minimize all potential hazards.

For the study of all important variables, the software AQ_Simu was developed allowing to conclude, in terms of simulated environment, a singular perspective on the effects to which any metallic networks are submitted, taking into account the RMS values of the magnetic induction field. Magnetic induction field values must be controlled in order to avoid reaching values higher than those referenced by ICNIRP and with this, to ensure the safety of people and the installation.

The influence of several constituent parameters of the installation for the increasing temperature were studied. Thus, for each of these parameters the following conclusions can be stated:

- 1) As far as the distance between the busbars is concerned, the greater the distance between the busbars, the higher the magnetic induction field originated in the metallic protection net. The increase in field strength leads to higher Joule losses in the metallic net and consequent increase in temperature;
- 2) In terms of the distance of the busbars to the metallic grids, as expected, a decrease in this distance leads to an increase in both the maximum RMS value of magnetic induction field and the dissipated power (consequent increase in temperature);
- 3) As for the size of each square of the grid, when they increase, it causes induced currents to be generated, which are directly related to the heating of metallic networks. Therefore, it is very important in terms of the safety of people and the installation that networks have large squares. In this case, the increase in losses due to Joule effect and the associated heating is avoided;
- 4) Considering the diameter of the conductors of the networks, also as would be expected, the larger the diameter of the conductors, the greater the losses due to Joule effect. In fact, by increasing the cross-section of the metallic conductors the equivalent electrical resistance decreases, whereby the induced electric current increases. As the losses are proportional to the square of the induced currents it will result in higher the heating values;
- 5) The existence of a varnished/plastic cover in the conductors of the metallic protection grid is an important factor, promoting an electrical insulation of the conductor to external phenomena, where even high currents can circulate. However, the existence of this protection leads

to an increase in the temperature inside the conductor. As there are more layers for the thermal effect in the conductors of the network and given the fact that plastic cover is considered an insulator, this solution has advantages for the safety of people and preservation for the conductive material;

- 6) The choice of materials that constitute the metallic protection nets is essential and takes into account all the studies demonstrated here, since they influence them directly. Therefore, high resistivity materials should prevail as they inhibit the formation of induced currents. This reduces the heat generated and still increases the safety of people.

A. Future work

The purpose of this work was to model the effects associated with thermal and magnetic study in a network and/or metallic doors, always with the precept of people and facilities safety.

Considering this theme as important in the elaboration of any primary and exclusive thermal study, this work can evolve even more in this sense, becoming an essential tool.

Therefore, the study of optimization for each variable that influences in the adjustment of thermal effect can be modeled, in order to meet the best efficiency ratio in the installation, never compromising the safety of people.

In this sense, given the evolution in optimization methods, it is possible in this case, given the nominal current of the main buses, to perform an automatic study that produces results on the cost effectiveness of the installation versus the safety of people and materials. These automatic values would surely give answer to even more cases, namely the distance between buses, the distance to the grids/doors taking into account the size of the grid, conductors sections, thicknesses and also any plastic/varnished coverings.

REFERENCES

- [1] V. Rudnev, D. Loveless, R. Cook, and M. Black, *Handbook of Induction Heating*. Marcel Dekker, Inc, 2003.
- [2] K. Gupta and N. Gupta, *Advanced Electrical and Electronics Materials: Processes and Applications*. Scrivener Publishing LLC., 2015.
- [3] J. L. Dosset and H. E. Boyer, *Practical Heat Treating*. ASM International, second edition ed., 2006.
- [4] I. C. on Non-Ionizing Radiation, *ICNIRP guidelines: For limiting exposure to time-varying electric and magnetic fields (1Hz-100kHz)*.
- [5] J. L. C. Pinto de Sa, *Guia de mitigacao da emissao de campo magnetico a 50Hz em instalaes da EDP*.
- [6] J. A. B. Faria, *Electromagnetic Foundations of Electrical Engineering*. John Wiley and Sons, Ltd., 2008.
- [7] T. Modric, S. Vujevic, and D. Lovric, "3d computation of the power lines magnetic field," pp. 1-9.
- [8] P. Zegarmistrz, S. Mitkowski, A. Porebska, and A. Dabrowski, "Nodal analysis of finite square resistive grids and the teaching effectiveness of students projects," pp. 84-89.
- [9] P. Talukda, *1D Steady State Heat Conduction*. NIIT Delhi.
- [10] M. Massoud, *Engineering Thermofluids: Thermodynamics, Fluid Mechanics, and Heat Transfer*. 2005.
- [11] T. MathWorks, *Matlab 2015a*. Natick, Massachusetts, United States.